PROCEEDINGS A

rspa.royalsocietypublishing.org

Research

Cite this article: Lafont T, Totaro N, Le Bot A. 2017 Coupling strength assumption in statistical energy analysis. *Proc. R. Soc. A* **473**: 20160927.
http://dx.doi.org/10.1098/rspa.2016.0927

Received: 20 December 2016
Accepted: 17 March 2017

Subject Areas:
structural engineering, acoustics, wave motion

Keywords:
sound and vibration, statistical energy analysis, weak coupling

Author for correspondence:
A. Le Bot
e-mail: alain.le-bot@ec-lyon.fr

Electronic supplementary material is available online at https://dx.doi.org/10.6084/m9.figshare.c.3732244.

THE ROYAL SOCIETY PUBLISHING

Coupling strength assumption in statistical energy analysis

T. Lafont[1,2], N. Totaro[1] and A. Le Bot[2]

[1]Laboratoire de Tribologie et Dynamique des Systèmes, École Centrale de Lyon, 69134 Écully, France
[2]Laboratoire Vibrations Acoustique, INSA Lyon, 69621 Villeurbanne, France

ALB, 0000-0002-3834-2685

This paper is a discussion of the hypothesis of weak coupling in statistical energy analysis (SEA). The examples of coupled oscillators and statistical ensembles of coupled plates excited by broadband random forces are discussed. In each case, a reference calculation is compared with the SEA calculation. First, it is shown that the main SEA relation, the coupling power proportionality, is always valid for two oscillators irrespective of the coupling strength. But the case of three subsystems, consisting of oscillators or ensembles of plates, indicates that the coupling power proportionality fails when the coupling is strong. Strong coupling leads to non-zero indirect coupling loss factors and, sometimes, even to a reversal of the energy flow direction from low to high vibrational temperature.

1. Introduction

Statistical energy analysis [1,2] (SEA) is a well-known statistical theory of sound and vibration based on an estimation of energy transfer between subsystems subjected to random forces. The main result is the so-called coupling power proportionality, which states that the power transmitted between any pair of coupled oscillators submitted to uncorrelated white noise forces is proportional to the difference in their energies [3]. A generalization to an arbitrary number of oscillators was achieved by Newland [4] with the additional hypothesis that the coupling is weak. For multi-degree of freedom subsystems, the coupling power proportionality is still valid (but now with the difference in modal energies) but requires further assumptions (rain-on-the-roof excitations, light damping, large number of resonant modes). The reader

may refer to [5–11] for reviews of SEA and discussions on the required hypotheses.

The question of coupling in SEA has been the subject of numerous discussions in the literature. It is generally understood that the coupling power proportionality is verified when the coupling between subsystems is weak and conservative. The assumption of conservative coupling is implicitly satisfied with the three types of classical coupling: elastic, gyroscopic and inertial. When dissipation occurs in couplings, the coupling power proportionality generally fails because the exchanged power is a linear combination of the vibrational energies, which does not reduce to a difference of energies [12].

The status of weak coupling is more disparate. In [3], weak coupling was invoked to derive the coupling power proportionality between two oscillators. But in [13], the assumption was relaxed without modifying the result. In [4], the weak coupling is again invoked through the perturbation technique to generalize the coupling power proportionality to more than two oscillators. When the number of oscillators is greater than two, a strong coupling invalidates the coupling power proportionality. A counter-example with three resonators is given in [14]. The exchanged power is found to be a linear combination of the energies of all the oscillators and not only the two adjacent ones. The importance of weak coupling for SEA applied to sets of mechanical resonators has been underlined in [15], while Keane & Price [16] suggest that strong coupling may be acceptable in SEA for two point-connected subsystems but with coupling loss factors not given in a closed form.

Several authors have proposed weak coupling criteria. A review is given by Finnveden [17]. Smith [18] studied the transition from weak to strong coupling and established a criterion based on the ratio of the coupling loss factor and the damping loss factor. The coupling is said to be strong if the subsystem has a damping loss factor smaller than the coupling loss factor. Langley [19] put forward a definition of weak coupling based on Green's functions: the coupling is weak if the Green function of the uncoupled subsystem is approximately equal to the Green function of the coupled system. The weak coupling indicator of Fahy & James [20] relies on Langley's definition. The quantification of coupling is achieved by estimating the rising time θ of energy of the indirectly excited subsystem. When the ratio between θ and the signal duration is small compared with unity, the coupling is weak. Mace [21] found, by a wave approach, that two parameters based on reflectance, reflection and transmission coefficients are necessary to estimate the coupling strength. See also [22], where a distinction is made between the strength of the connection and the strength of the coupling. Finnveden [23] showed that the coupling power proportionality is valid for three subsystems, provided that a factor noted as γ (the ratio of conductivity and the product of modal overlaps) is small.

This study is a discussion on the necessity of the weak coupling assumption in SEA. It aims to provide numerical evidence that SEA is fundamentally based on the assumption of weak coupling. Two facts are examined: the principle of the coupling power proportionality and the exactness of the proportionality constant predicted by classical SEA. The paper is organized as follows. Section 2 focuses on a discussion on mechanical oscillators, while §3 is dedicated to coupled plates with resonators. In both sections, an SEA prediction is compared with a reference calculation systematically in weak and strong coupling regimes. The reasons for the discrepancy in the strong regime are discussed. Finally, some concluding remarks are given in the last section.

2. Coupled oscillators

(a) Statistical energy analysis for coupled oscillators

Consider two oscillators of mass m_i attached to a rigid frame by springs of stiffness k_i, a dashpot with a viscous damping coefficient λ_i and coupled together through a spring of stiffness K, as shown in figure 1*a*. The oscillators are submitted to external forces F_i. Assuming that the elastic coupling is conservative and that the external forces are stationary and uncorrelated white noise, it is known [3,13] that the mean power exchanged between subsystems i and j is proportional to

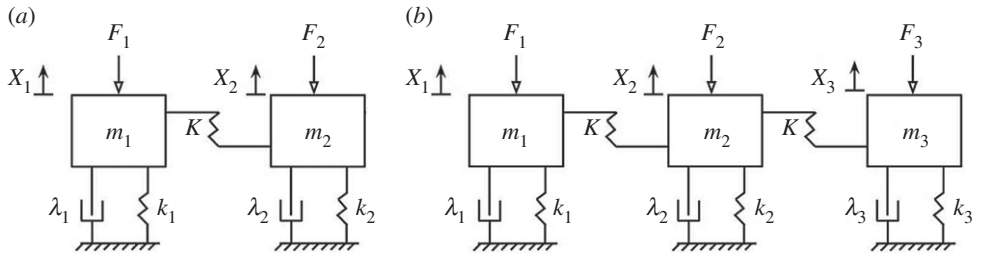

Figure 1. Mechanical oscillators submitted to uncorrelated random forces F_i. (*a*) Two oscillators and (*b*) three oscillators.

the difference in the mean vibrational energies

$$P_{ij} = \beta(E_i - E_j), \tag{2.1}$$

where P_{ij}, E_i, E_j are the random expectations of the exchanged power and vibrational energies. This is the so-called coupling power proportionality. For an elastic coupling, the coefficient β is

$$\beta = \frac{K^2(\Delta_i + \Delta_j)}{m_i m_j[(\omega_i^2 - \omega_j^2)^2 + (\Delta_i + \Delta_j)(\Delta_i\omega_j^2 + \Delta_j\omega_i^2)]}, \tag{2.2}$$

where $\Delta_i = \lambda_i/m_i$ is the half power bandwidth and $\omega_i = [(k_i + K)/m_i]^{1/2}$ is the 'blocked' natural frequency of oscillator i.

The coupling power proportionality (2.1) and the coefficient β of equation (2.2) are valid under quite general conditions. The only required assumption is that the forces F_1 and F_2 have constant power spectral densities S_1 and S_2 and a zero cross-power spectral density. Although the assumption of weak coupling was invoked in the original publication [3], it has been relaxed in the second publication [13]. The coupling power proportionality between two oscillators is therefore established for weak and strong coupling irrespective of the level of dissipation.

The coupling power proportionality remains verified to good approximation if, instead of a true white noise, the external forces are band limited, provided that the two 'blocked' frequencies are contained in the frequency band of excitation. In that case, we may introduce the central frequency of excitation ω_c and the usage is to decompose the coefficient β in the product $\beta = \eta_{ij}\omega_c$, where η_{ij} is the coupling loss factor. The symmetry of β under the permutation $i \leftrightarrow j$ allows to write

$$\eta_{ij}\omega_c = \eta_{ji}\omega_c. \tag{2.3}$$

This reciprocity relationship is also called the consistency condition [24].

The coupling power proportionality is valid for more than two oscillators, in which case it applies to any pair of oscillators. But the original method [3] gives rise to tedious calculations for more than two oscillators. The perturbation technique introduced by Newland [4] gives a satisfactory solution to this problem, but requires the additional assumption of weak coupling. The final result is that equation (2.1) is valid up to order 2 in the power of coupling strength. The coefficient β is again given by (2.2), except that the frequencies $\omega_i = (k_i/m_i)^{1/2}$ are now the 'free' natural frequencies. In the weak coupling regime $K \ll k_i$, the 'blocked' and 'free' natural frequencies are equal at first order in K/k_i, and therefore the 'free' and 'blocked' versions of β are equal at second order in K/k_i. The question of whether the factor β must be used with the free or blocked natural frequencies is therefore irrelevant in the weak coupling regime but may have a certain importance when the coupling starts to strengthen.

Let us now introduce the example of mechanical resonators that will serve as a numerical test to discuss these general ideas further. We consider three oscillators coupled by springs of stiffness

K and excited by uncorrelated white noise forces, as shown in figure 1*b*. Taking into account the coupling power proportionality, the energy balance of each oscillator reads

$$P_i = \omega_c \eta_i E_i + \omega_c \sum_{j \neq i} (\eta_{ij} E_i - \eta_{ji} E_j), \tag{2.4}$$

where P_i denotes the mean power supplied by the force F_i, $\eta_i \omega_c E_i$ is the mean power dissipated in the dashpot and $\eta_i = \lambda_i/(m_i \omega_c)$ is the damping loss factor. In the case of figure 1*b*, these equations may be written in a matrix form

$$\begin{bmatrix} P_1 \\ P_2 \\ P_3 \end{bmatrix} = \omega_c \begin{bmatrix} \eta_1 + \eta_{12} & -\eta_{21} & 0 \\ -\eta_{12} & \eta_2 + \eta_{21} + \eta_{23} & -\eta_{32} \\ 0 & -\eta_{23} & \eta_3 + \eta_{32} \end{bmatrix} \begin{bmatrix} E_1 \\ E_2 \\ E_3 \end{bmatrix}. \tag{2.5}$$

The above coupling loss factor matrix verifies the conditions of energy balance and consistency. Since there is no physical link between oscillators 1 and 3, the coupling loss factors η_{13} and η_{31} are set to zero. Such a system is referred to as a proper-SEA system [25].

(b) Reference calculation for coupled oscillators

We now examine the reference calculation for the example of three oscillators.

In the Fourier space, the equations of motion of coupled oscillators are $\mathbf{DX} = \mathbf{F}$, where $\mathbf{X}$ is a vector whose components are the displacements of oscillators, $\mathbf{F}$ is the external force vector and $\mathbf{D}$ is the dynamic stiffness matrix. The frequency response matrix $\mathbf{H}$, obtained by inverting $\mathbf{D}$, of the mechanical oscillators of figure 1 is

$$\mathbf{H}(\omega) = \begin{bmatrix} m_1(\omega_1^2 - \omega^2 + \mathrm{j}\omega\Delta_1) & -K & 0 \\ -K & m_2(\omega_2^2 - \omega^2 + \mathrm{j}\omega\Delta_2) & -K \\ 0 & -K & m_3(\omega_3^2 - \omega^2 + \mathrm{j}\omega\Delta_3) \end{bmatrix}^{-1}, \tag{2.6}$$

where $\omega_i = [(k_i + K)/m_i]^{1/2}$ is the 'blocked' natural frequency of oscillators $i = 1, 3$, $\omega_2 = [(k_2 + 2K)/m_2]^{1/2}$ is that of oscillator 2 and $j = \sqrt{-1}$ is the imaginary unit.

The frequency response matrix, also called the receptance matrix, gives the response $\mathbf{X}$ of the system to any harmonic input $\mathbf{F}$ by $\mathbf{X} = \mathbf{HF}$. But when the forces $\mathbf{F}$ are random, the response $\mathbf{X}$ is also random and the question is rather how to determine the output power spectral densities $S_{X_i X_j}$ from the knowledge of the input power spectral densities $S_{F_i F_j}$. The theory of random vibrations shows that $S_{X_i X_j} = \sum_{k,l} \bar{H}_{ik} H_{jl} S_{F_k F_l}$, where H_{ik} is the entry of row i and column k in the receptance matrix $\mathbf{H}$ and the overline denotes the complex conjugate. For the power spectrum of the velocity $S_{\dot{X}_i \dot{X}_j}$, the receptance H_{ik} is simply replaced by $j\omega H_{ik}$ and H_{jl} by $j\omega H_{jl}$. For the cross-power spectrum $S_{F_i \dot{X}_j}$ of force F_i and velocity $\dot{X}_j$, H_{ik} is replaced by 1 and H_{jl} by $\mathrm{j}\omega H_{jl}$. All other combinations are possible. The probabilistic expectation of a product $X_i X_j$, $\dot{X}_i \dot{X}_j$ or $F_i \dot{X}_j$ is simply obtained by integration of the power spectrum over all frequencies. For instance, $\langle X_i X_j \rangle = \int S_{X_i X_j} \, \mathrm{d}\omega/2\pi$, where $\langle . \rangle$ denotes the probability expectation or mean value.

When the forces F_k are random, stationary and uncorrelated with a power spectral density S_k constant within the frequency band $[\omega_{\min}, \omega_{\max}]$ and zero elsewhere, the expectation of the velocity square of oscillator i is

$$\langle \dot{X}_i^2 \rangle = \sum_k \frac{S_k}{\pi} \int_{\omega_{\min}}^{\omega_{\max}} \omega^2 |H_{ik}(\omega)|^2 \, \mathrm{d}\omega, \tag{2.7}$$

where we have used $\mathbf{H}(-\omega) = \bar{\mathbf{H}}(\omega)$ and the fact that $S_{F_k F_l} = 0$ when $k \neq l$. Considering that the mean vibrational energy E_i is defined as twice the mean kinetic energy, we get

$$E_i = \sum_k \frac{S_k}{\pi} \int_{\omega_{\min}}^{\omega_{\max}} m_i \omega^2 |H_{ik}(\omega)|^2 \, \mathrm{d}\omega. \tag{2.8}$$

In the same way, the mean product $\langle X_i \dot{X}_j \rangle$ is

$$\langle X_i \dot{X}_j \rangle = \sum_k \frac{S_k}{\pi} \int_{\omega_{\min}}^{\omega_{\max}} \mathrm{Re}[j\omega \bar{H}_{ik}(\omega) H_{jk}(\omega)] \, \mathrm{d}\omega, \tag{2.9}$$

where Re denotes the real part of a complex number. The net power $P_{ij} = K\langle X_i \dot{X}_j \rangle$ transmitted from oscillator i to oscillator j is therefore

$$P_{ij} = K \sum_k \frac{S_k}{\pi} \int_{\omega_{\min}}^{\omega_{\max}} \mathrm{Re}[j\omega \bar{H}_{ik}(\omega) H_{jk}(\omega)] \, \mathrm{d}\omega. \tag{2.10}$$

One may observe from equation (2.6) that this sum is zero for P_{13}.

The mean power injected into oscillator i is

$$P_i = \langle F_i \dot{X}_i \rangle = \frac{S_i}{\pi} \int_{\omega_{\min}}^{\omega_{\max}} \mathrm{Re}[j\omega H_{ii}(\omega)] \, \mathrm{d}\omega. \tag{2.11}$$

Thus, by equations (2.8), (2.10) and (2.11), the numerical computation of the expectations of the vibrational energies, transmitted power and supplied power reduces to a frequency integration of the products of the frequency response functions.

(c) Non-constrained identification technique

The power injection method introduced by Lyon [1] and Bies & Hamid [26] is a technique to identify the coupling loss factors appearing in equation (2.5) by testing the structure. It is usually employed when a direct estimation of the coupling loss factors is not possible. It consists in exciting successively each oscillator and computing (or measuring in the original method) the resulting energies and supplied power in all other oscillators.

Let us fix k the index of an oscillator and let us denote by E_i^k the vibrational energy of oscillator i when only oscillator k is excited with a supplied power P_k. Application of equation (2.5) gives three linear equations on the coupling loss factors η_{ij} and damping loss factors η_i. This procedure, repeated for all k, gives a system $\mathbf{P} = \mathbf{EN}$, where $\mathbf{P}$ is the injected power vector, $\mathbf{E}$ is a matrix composed of vibrational energies E_i^k and $\mathbf{N}$ is a vector which contains the damping loss factors and coupling loss factors without prejudging that some of them are zero. In the case of the three oscillators of figure 1, it yields

$$\begin{bmatrix} P_1 \\ 0 \\ 0 \\ 0 \\ P_2 \\ 0 \\ 0 \\ 0 \\ P_3 \end{bmatrix} = \omega_c \begin{bmatrix} E_1^1 & E_1^1 & E_1^1 & -E_2^1 & 0 & 0 & -E_3^1 & 0 & 0 \\ 0 & -E_1^1 & 0 & E_2^1 & E_2^1 & E_2^1 & 0 & -E_3^1 & 0 \\ 0 & 0 & -E_1^1 & 0 & 0 & -E_2^1 & E_3^1 & E_3^1 & E_3^1 \\ E_1^2 & E_1^2 & E_1^2 & -E_2^2 & 0 & 0 & -E_3^2 & 0 & 0 \\ 0 & -E_1^2 & 0 & E_2^2 & E_2^2 & E_2^2 & 0 & -E_3^2 & 0 \\ 0 & 0 & -E_1^2 & 0 & 0 & -E_2^2 & E_3^2 & E_3^2 & E_3^2 \\ E_1^3 & E_1^3 & E_1^3 & -E_2^3 & 0 & 0 & -E_3^3 & 0 & 0 \\ 0 & -E_1^3 & 0 & E_2^3 & E_2^3 & E_2^3 & 0 & -E_3^3 & 0 \\ 0 & 0 & -E_1^3 & 0 & 0 & -E_2^3 & E_3^3 & E_3^3 & E_3^3 \end{bmatrix} \begin{bmatrix} \eta_1 \\ \eta_{12} \\ \eta_{13} \\ \eta_{21} \\ \eta_2 \\ \eta_{23} \\ \eta_{31} \\ \eta_{32} \\ \eta_3 \end{bmatrix}. \tag{2.12}$$

As the vector $\mathbf{P}$ and the matrix $\mathbf{E}$ are assumed to be known, the vector $\mathbf{N}$ is computed by solving equation (2.12).

Note that the two terms η_{13} and η_{31} are not forced to be zero in this procedure. It may be that non-zero values of η_{13} and η_{31} are obtained with the power injection method. These terms are called indirect coupling loss factors because their existence suggests that energy flows directly from oscillator 1 to oscillator 3 even though they are uncoupled.

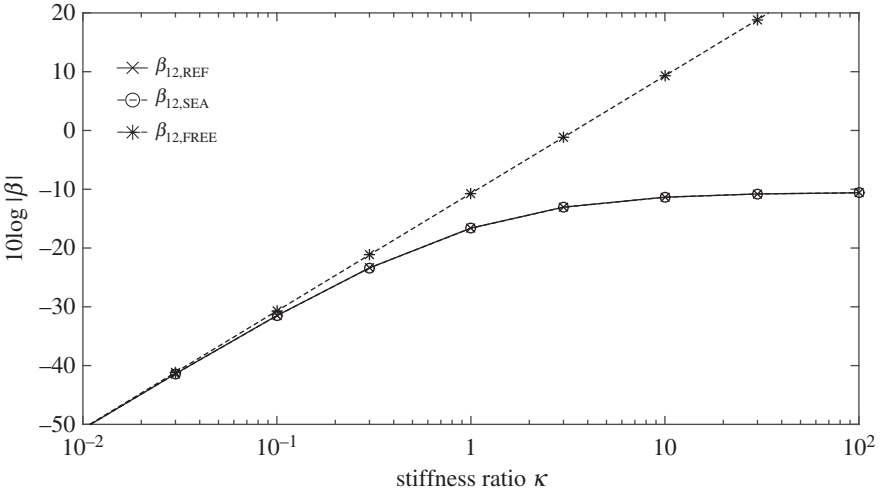

Figure 2. Evolution of $\beta_{12,\mathrm{REF}}$, $\beta_{12,\mathrm{SEA}}$ and $\beta_{12,\mathrm{FREE}}$ for two oscillators versus the stiffness ratio κ.

Table 1. Parameters of the mechanical oscillators.

oscillator	mass m_i (kg)	stiffness k_i (N m^{-1})	damping λ_i (Ns m^{-1})
1	1.0	1.0	0.1
2	4.0	1.0	0.4
3	2.0	1.0	0.2

(d) Comparison between statistical energy analysis and reference

To compare the prediction of SEA with results from the reference calculation, we fix the input power spectral densities $S_1 = 1$ and $S_2 = S_3 = 0$.

The reference calculation consists in computing first the frequency response matrix $\mathbf{H}(\omega)$ by equation (2.6), then the mean vibrational energies E_i by equation (2.8) and finally the transmitted power P_{ij} by equation (2.10). The ratio between the transmitted power P_{ij} and the difference of energies $E_i - E_j$ is noted by $\beta_{ij,\mathrm{REF}}$.

The SEA calculation consists in calculating the coupling loss factors directly by equation (2.2) with the 'blocked' natural frequencies. The obtained value of the coefficient β is noted by $\beta_{ij,\mathrm{SEA}}$. If the 'free' natural frequencies are used instead, the resulting factor shall be denoted by $\beta_{ij,\mathrm{FREE}}$. We then compare $\beta_{ij,\mathrm{SEA}}$, $\beta_{ij,\mathrm{FREE}}$ and $\beta_{ij,\mathrm{REF}}$ for a varying coupling strength.

The mechanical characteristics of the oscillators are given in table 1. All stiffnesses k_i are fixed to 1 arbitrarily. The viscous damping coefficient λ_i is proportional to the mass m_i so that the half power bandwidth $\Delta_i = \lambda_i/m_i = 0.1$ is the same for all oscillators. The stiffness ratio $\kappa = K/\sqrt{k_i k_j}$ varies from 0.01 to 100. As $k_1 = k_2 = k_3$ in the numerical simulation, there is a unique value of κ for the two pairs of oscillators. The blocked natural frequencies, affected by κ, are constant in weak coupling but increase when the coupling strengthens. The frequency bandwidth of integration is taken sufficiently large as $\omega_{\min} = 0$ and $\omega_{\max} = 10 \times \omega_{\mathrm{m}}$, where ω_{m} is the largest blocked frequency. The central frequency is fixed to $\omega_{\mathrm{c}} = 0.736\,\mathrm{rad\,s^{-1}}$, which is the mean value of free natural frequencies.

(i) Two coupled oscillators

First, let us present results in the case of the two oscillators shown in figure 1*a*. Figure 2 shows the evolution of $\beta_{12,\mathrm{SEA}}$, $\beta_{12,\mathrm{FREE}}$ and $\beta_{12,\mathrm{REF}}$ versus the stiffness ratio κ.

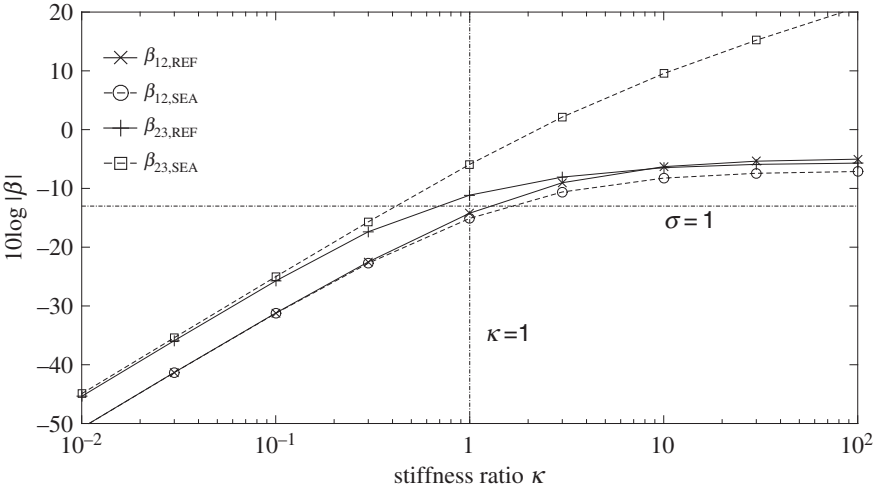

Figure 3. Evolution of $\beta_{ij,REF}$ and $\beta_{ij,SEA}$ for three oscillators versus the stiffness ratio κ.

A perfect agreement between $\beta_{12,SEA}$ and $\beta_{12,REF}$ is observed for any strength of coupling. For two coupled oscillators excited by random forces, the coupling power proportionality holds irrespective of the coupling strength.

Instead of using the 'blocked' natural frequencies in equation (2.2) one may use the 'free' natural frequencies in equation (2.2). The resulting factor noted $\beta_{12,FREE}$ is also shown in figure 2. It appears that $\beta_{12,FREE}$ and $\beta_{12,SEA}$ agree well for weak coupling but the discrepancy emerges rapidly for $\kappa > 1$. It is apparent from figure 2 that the correct expression of β is therefore obtained with the 'blocked' natural frequencies and that the usage of 'free' natural frequencies is limited to weak coupling.

(ii) Three coupled oscillators

Next, let us consider the case of the three oscillators shown in figure 1*b*.

Figure 3 shows the evolution of $\beta_{ij,SEA}$ and $\beta_{ij,REF}$ between oscillators 1 and 2 and between oscillators 2 and 3 when oscillator 1 is excited by a white noise force. One may observe that the β_{12} values calculated by both methods are in good agreement until a threshold value of the stiffness ratio about unity. Beyond this value, $\beta_{12,REF}$ and $\beta_{12,SEA}$ disagree by several dBs, indicating that equation (2.2) is no longer valid in the strong coupling regime. Results with β_{23} confirm these observations. The discrepancy is even more obvious in strong coupling since the error may reach several orders of magnitude.

The Smith criterion [18] states that strong coupling starts when the ratio of the coupling loss η_{ij} factor to the damping loss factor η_i is greater than 1. In the present notations, Smith's ratio is $\sigma = (\beta_{ij}/\Delta_i + \beta_{ji}/\Delta_j)$. The β_{ij} that must be used in this criterion is $\beta_{ij,SEA}$, predicted by SEA, and not $\beta_{ij,REF}$, which cannot be estimated in general. The horizontal dashed line labelled $\sigma = 1$ in figure 3 gives the limit value $(\Delta_i^{-1} + \Delta_j^{-1})^{-1}$ of β_{ij} separating weak and strong regimes. As $\Delta_1 = \Delta_2 = \Delta_3$ in the present simulation, this threshold is the same for the two couplings. When $\beta_{ij,SEA}$ exceeds this level, the coupling regime is strong and errors start to appear between $\beta_{ij,SEA}$ and $\beta_{ij,REF}$.

From these results, one can clearly draw a separation between weak and strong coupling. This threshold, estimated at $\kappa \sim 1$ or $\sigma \sim 1$ in the present simulation, is sufficient to observe the failure of the coupling power proportionality. The assumption of weak coupling is necessary to accurately apply SEA in the case of three or more oscillators although it was not necessary for two oscillators. The case of two resonators is therefore a special case which is by no means representative of the general case.

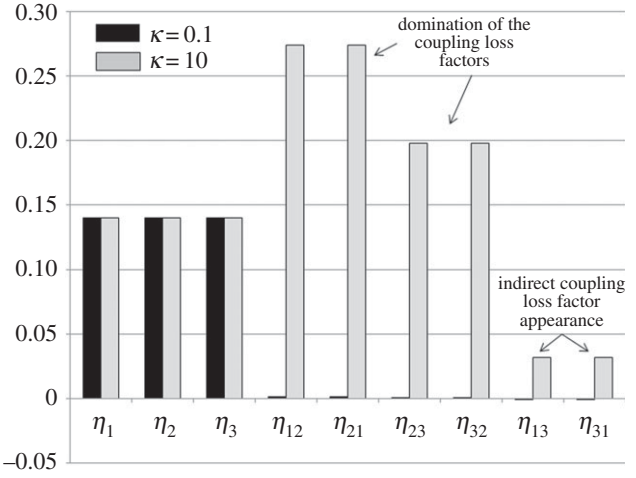

Figure 4. Identified damping loss factors and coupling loss factors for weak coupling ($\kappa = 0.1$) and strong coupling ($\kappa = 10$).

Table 2. Damping and coupling loss factors identified by the non-constraint method.

κ	η_1	η_2	η_3	η_{12}	η_{21}	η_{23}	η_{32}	η_{13}	η_{31}
0.01	0.14	0.14	0.14	1.2×10^{-5}	1.2×10^{-5}	4.4×10^{-5}	4.4×10^{-5}	-3.8×10^{-10}	-3.8×10^{-10}
0.1	0.14	0.14	0.14	1.0×10^{-3}	1.0×10^{-3}	4.4×10^{-5}	4.4×10^{-5}	-4.2×10^{-6}	-4.2×10^{-6}
1	0.14	0.14	0.14	5.8×10^{-2}	5.8×10^{-2}	0.147	0.147	-5.6×10^{-3}	-5.6×10^{-3}
10	0.14	0.14	0.14	0.274	0.274	0.198	0.198	0.032	0.032
100	0.14	0.14	0.14	0.333	0.333	0.174	0.174	0.063	0.063

(iii) Indirect coupling

Indirect coupling may appear when the coupling threshold is exceeded. To highlight this phenomenon, the non-constrained identification technique is used jointly with the reference calculation to provide the exact oscillator energies and supplied powers. The vector $\mathbf{N}$ is computed for different coupling strengths by using the energies and powers calculated by equations (2.8) and (2.11). If the coupling power proportionality (2.1) and equation (2.2) are valid one expects to find a coupling loss factor matrix of a proper-SEA [25]: the indirect coupling loss factors must be zero and consistency is respected.

The oscillators are successively excited with power spectral densities $S_i = 1$ over the frequency band $0–10 \times \omega_m$ rad s^{-1}. The loss factors are computed with equation (2.12) for several values of κ ranging from 0.01 and 100.

Table 2 shows the values of the identified loss factors versus the stiffness ratio. Figure 4 represents the damping and coupling loss factors in the form of a bar chart for two stiffness ratios, 0.1 and 10.

Various comments can be made. Firstly, the identified damping loss factors do not vary with the coupling strength. Their values are well estimated compared with the prescribed value $\eta_i = \Delta_i/\omega_c = 0.14$. The power injection method gives the correct values of the damping loss factors in all cases of coupling.

Secondly, comparing, respectively, η_{12} with η_{21} and η_{23} with η_{32} in figure 4 we may observe that $\eta_{12} = \eta_{21}$ and $\eta_{23} = \eta_{32}$ in all cases. Consistency is therefore always verified in both the weak and strong coupling regimes.

Thirdly, the indirect coupling loss factors η_{13}, η_{31} are negligible compared with other coupling loss factors in weak coupling (table 2). For a coupling ratio of 0.1 as in figure 4, the indirect

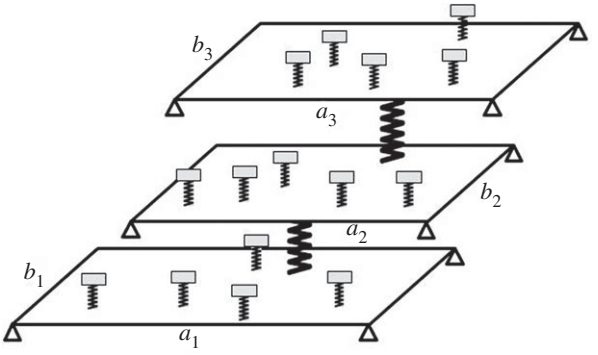

Figure 5. Simply supported plates with random resonators and coupled by springs.

coupling loss factors are negligible. The identified coupling loss factor matrix is therefore a proper-SEA matrix. But when the coupling strength approaches the threshold value indirect coupling starts to appear. For a coupling strength greater than the threshold value (figure 4), the indirect coupling loss factors become important and the coupling loss factor matrix is no longer a proper-SEA matrix.

The non-constrained identification technique highlights the appearance of indirect coupling and its importance when the coupling is strong. The indirect coupling loss factors may even dominate the energy exchanges. A correct prediction of the energy exchanges in strong coupling therefore requires that the indirect coupling loss factors are taken into account.

3. Coupled plates

In this section, we discuss the example of three simply supported rectangular plates with random resonators and coupled by springs.

(a) Statistical energy analysis for coupled plates

Let us consider three plates with resonators and coupled by springs of stiffness K, as shown in figure 5. The three plates are referenced by $i = 1, 2, 3$. The plates are rectangular and have length a_i and width b_i. Random resonators are positioned on each plate. The bending stiffness of the plates is noted as D_i, the mass per unit area m_i and the modal density n_i. The asymptotic expression of the modal density in the plates is [2]

$$n_i = \frac{a_i b_i}{4\pi}\sqrt{\frac{m_i}{D_i}}. \tag{3.1}$$

According to SEA, assuming that the first plate is driven by a single random force with a constant power spectral density and that the frequency band centred in ω_c contains a sufficiently large number of modes, the expectation of the power exchanged between plates i and j is

$$P_{ij} = \beta\left(\frac{E_i}{n_i} - \frac{E_j}{n_j}\right), \tag{3.2}$$

where E_i is the mean vibrational energy of plate i. This is the coupling power proportionality for plates. The proportionality now holds with the difference of modal densities $T_i = E_i/n_i$ that we shall call vibrational temperatures.

The coupling loss factor for spring coupled subsystems has been given from the former texts on SEA (see for instance [27], eqn (25)). The classical formula is $\eta_{ij} = \pi K^2 n_j / 2\omega_c^3 m_i' m_j'$, where m_i' is

the mass of subsystem i. The coefficient $\beta = \omega_c n_i \eta_{ij} = \omega_c n_j \eta_{ji}$ for two plates coupled by a spring of stiffness K is therefore [22]

$$\beta = \frac{K^2}{32\pi\omega_c^2} \frac{1}{\sqrt{m_i D_i}\sqrt{m_j D_j}}. \tag{3.3}$$

The consistency relationship $n_i\eta_{ij} = n_j\eta_{ji}$ comes from the symmetry of β under the permutation $i \leftrightarrow j$. With this convention, the coupling power proportionality reads

$$P_{ij} = \omega_c(\eta_{ij}E_i - \eta_{ji}E_j). \tag{3.4}$$

The energy balance (2.4) applies. Consequently, SEA leads to equation (2.5) for the example of figure 5 for exactly the same reasons as for the three oscillators case. Formally, the problem of coupled plates is similar to that of coupled oscillators except for the calculation of coupling loss factors.

Since we have assumed that only plate 1 is excited, we may set $P_2 = P_3 = 0$ in equation (2.5). By a direct calculation, the ratios of modal energies $T_i = E_i/n_i$ predicted by SEA are

$$\frac{T_2}{T_1} = \frac{\eta_{12}}{[(\eta_2 + \eta_{21} + \eta_{23}) - \eta_{32}(\eta_{23}/(\eta_3 + \eta_{32})]} \times \frac{n_1}{n_2} \tag{3.5}$$

and

$$\frac{T_3}{T_2} = \frac{\eta_{23}}{\eta_3 + \eta_{32}} \times \frac{n_2}{n_3}. \tag{3.6}$$

These equations will be used as a test of the SEA prediction.

(b) Reference calculation for coupled plates

In the reference calculation, plate 1 is excited by a single-point force at position x_0, y_0. The force field f has expression

$$f(x, y, t) = F(t)\delta(x - x_0)\delta(y - y_0), \tag{3.7}$$

where F is a random force with a power spectral density S_1 constant in the frequency band $[\omega_{\min}, \omega_{\max}]$.

The mean vibrational energy is twice the mean kinetic energy $E_i = \int m_i \langle \dot{v}_i^2 \rangle \, \mathrm{d}x \, \mathrm{d}y$, where v_i denotes the deflection of plate i and the probability expectation is noted with brackets. The integral is performed over the plate surface. The energies may be calculated by means of the receptance of the coupled plates. The deflection v_i of plate i at position x, y when plate 1 is excited by a harmonic point force at position x_0, y_0 is noted as $H_{i1}(x, y, x_0, y_0; \omega)$, where ω is the circular frequency. The mean vibrational energy in plate i becomes

$$E_i = \frac{S_1}{\pi} \int_0^{a_i} \int_0^{b_i} \int_{\omega_{\min}}^{\omega_{\max}} m_i \omega^2 |H_{i1}(x, y, x_0, y_0; \omega)|^2 \, \mathrm{d}\omega \, \mathrm{d}y \, \mathrm{d}x. \tag{3.8}$$

This equation is similar to equation (2.8) except that the difficulty now reduces to computing the receptances H_{ij} of the coupled plates. This problem is solved in appendix A.

The mean power flowing from subsystem i to subsystem j is $P_{ij} = K\langle v_i \dot{v}_j \rangle$, where v_i, v_j are the deflection of plates at the attachment point. In terms of receptances,

$$P_{ij} = K\frac{S_1}{\pi} \int_{\omega_{\min}}^{\omega_{\max}} \mathrm{Re}[j\omega \bar{H}_{i1}(\chi_i, \xi_i, x_0, y_0; \omega) H_{j1}(\chi_j, \xi_j, x_0, y_0; \omega)] \, \mathrm{d}\omega, \tag{3.9}$$

where χ_i, ξ_i are the coordinates of the attachment point on plate i.

In the reference calculation, the ratios T_2/T_1 and T_3/T_2 are obtained by computing the vibrational energies with equation (3.8) and the modal densities by equation (3.1).

Table 3. Geometrical parameters of the three plates.

plate	thickness (mm)	length (m)	width (m)
1	1	1	$1/\sqrt{3}$
2	1.5	$\sqrt{2}$	1
3	2.5	1	$\sqrt{3}$

Table 4. Positions of source and attachment points for the three plates.

plate	source	attachment 1–2	attachment 2–3
1	0.2×0.058	0.70×0.17	—
2	—	0.28×0.30	0.84×0.50
3	—	—	0.60×0.35

(c) Comparison between statistical energy analysis and reference

The parameters used for the numerical simulation are the following. The plates are made of steel with Young's modulus $E = 210\,\mathrm{GPa}$, density $7800\,\mathrm{kg\,m^{-3}}$ and Poisson coefficient $\nu = 0.3$, and the three damping loss factors are $\eta_1 = 0.001$, $\eta_2 = 0.001$ and $\eta_3 = 0.002$. The thickness, length and width are presented in table 3. They are chosen such that their ratios length/width are irrational in order to avoid regularity in the sequence of natural frequencies. The positions of the source point and spring attachment points are given in table 4. The frequency band is an octave centred on $\omega_c = 2\pi \times 2000\,\mathrm{rad\,s^{-1}}$ and the excitation is a single-point force applied to plate 1 with a constant power spectral density. The receptances are computed by taking into account all modes from 0 Hz to 5.7 kHz. The vibrational energies are estimated by choosing at random 50 receivers on each plate. The coupling stiffness K varies from $3 \times 10^3\,\mathrm{N\,m^{-1}}$ to $3 \times 10^7\,\mathrm{N\,m^{-1}}$.

Five resonators are placed on each plate. The total mass of the resonators does not exceed the total mass of each plate and their natural frequencies are randomly chosen within the frequency bandwidth of excitation. Their positions as well as their natural frequencies are chosen at random. The reference calculation is processed 44 times with different realizations of random resonators. Each sample of this population provides a result and their average value is compared with the SEA prediction of this statistical ensemble.

(i) Diffuse field

To check whether the vibrational field is diffuse in all plates, one must compute the mode count (the number of modes $N = n(\omega)(\omega_{\max} - \omega_{\min})$ in the frequency band of excitation) and wave attenuation. Table 5 shows that the mode count is of order of several hundreds for all plates, which is normally sufficiently high. To enforce diffuseness, attenuation must also be low to mix the energy efficiently by a large number of ray reflections [28]. Attenuation per mean free path is defined by $\eta\omega_c l/c_g$, where l is the mean free path and c_g is the group velocity of waves at frequency ω_c. The values of attenuation given in table 5 show that they are below 6% in all plates. A value of attenuation of about 0.03 means that rays reflect 30 times before losing 60% of their energy. These two conditions of high mode count and low attenuation are sufficient to ensure that energy fields are diffuse in the three plates [29]. Table 5 also summarizes the dimensionless wavelength (number of wavelengths in the mean free path), damping loss factor, mode count, attenuation per mean free path and modal overlap.

Figure 6 shows the positions of the plates in the dimensionless wavelength–damping loss factor plane. The isovalue lines indicate the relative standard deviation of the repartition of energy in plates observed by a reference calculation conducted on a single plate (see [10] for details). All plates are confined in the zone where the value of the relative standard deviation is less than

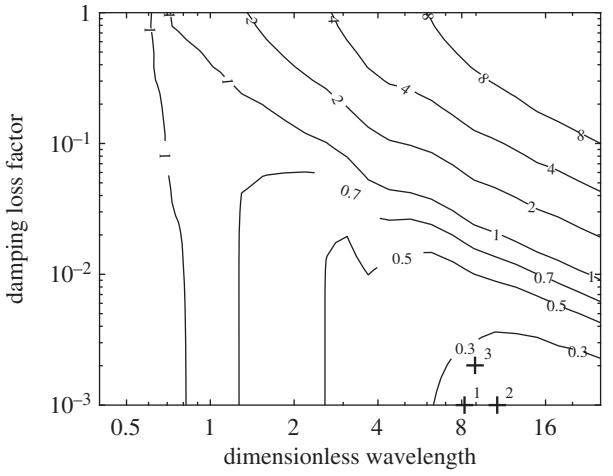

Figure 6. Isovalues of the relative standard deviation of energy in rectangular plates excited by a point force versus the dimensionless wavelength (wavelength per mean free path) and damping loss factor. Crosses indicate the actual positions of the plates.

Table 5. Dimensionless wavelength, damping loss factor, mode count, attenuation per mean free path and modal overlap of the plates.

plate	wavelength	damping	mode count	attenuation	modal overlap
1	8.2	0.001	368	0.026	0.4
2	10.7	0.001	600	0.034	0.6
3	9.0	0.002	441	0.056	0.9

0.3, meaning that the local fluctuations of energy within the plates are less than 30%. Because the actual value of the energy at the connecting points is different from the mean value predicted by SEA by less than 30%, one can expect that the error of SEA in the energy transfer is also less than 30%.

(ii) Energy exchange

Figure 7 shows a comparison between the values $\beta_{ij,\mathrm{SEA}}$ predicted by equation (3.3) and the numerical ratio $\beta_{ij,\mathrm{REF}} = P_{ij}/(E_i/n_i - E_j/n_j)$ obtained by the reference calculation. The coupling strength is controlled by the stiffness ratio $\kappa = K/\sqrt{m_i' m_j' \omega_c^4}$, where m_i' is the mass of plate i. As there are two couplings, there are two stiffness ratios. The horizontal scale of figure 7 indicates the maximal stiffness ratio which corresponds to the coupling between plates 1 and 2.

As in the case of coupled oscillators, $\beta_{ij,\mathrm{SEA}}$ is correct for low values of the stiffness ratio. This observation is valid for both pairs of plates. In the regime of weak coupling, the difference between $\beta_{ij,\mathrm{SEA}}$ and the average value of $\beta_{ij,\mathrm{REF}}$ is small. The grey zones of figure 7 indicate the fluctuations over the ensemble of 44 realizations. For all samples, the error is confined to a few decibels.

The weak coupling is a regime where the prediction of SEA is correct compared with reference calculations. In particular, since the sign of $\beta_{ij,\mathrm{REF}}$ is always found to be positive in the weak coupling regime, the energy flows from the oscillator with the highest vibrational temperature to the one with the lowest vibrational temperature.

The transition to strong coupling is governed by Smith's ratio, which is defined as the ratio of coupling and damping loss factors. This reads $\sigma = \beta_{ij}/M_i + \beta_{ji}/M_j$, where M_i is the modal overlap.

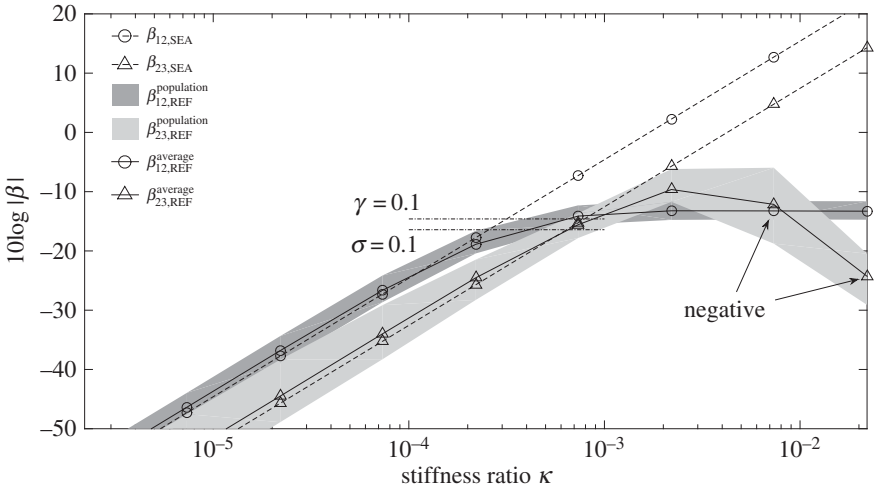

Figure 7. Evolution of $\beta_{ij,REF}$ and $\beta_{ij,SEA}$ for three plates versus the stiffness ratio κ of coupling 1–2.

A horizontal dashed line labelled $\sigma = 0.1$ is plotted in figure 7 to represent the limit level of β_{12} of the weak coupling regime for the first coupling (plates 1 and 2). It is apparent from figure 7 that the condition $\beta_{12} < 0.1\sigma$ predicts well the range of weak coupling where the error between SEA and the reference calculation is negligible. The level for coupling 2–3 is not represented in figure 7 but would predict a transition for a larger value of κ. The first coupling is therefore the most constraining one.

A second criterion for the transition is the so-called gamma factor. It is defined as $\gamma = 2\beta_{ij}/\pi M_i M_j$ [17]. This maximal level of β is plotted in figure 7 for coupling 1–2 as a horizontal line labelled $\gamma = 0.1$. It is clear from figure 7 that the criterion $\beta_{12} < 0.1\gamma$ also predicts well the transition. As previously, the second coupling is less restrictive and is not represented in figure 7.

However, it may be remarked that the value of the stiffness ratio κ never reaches 1, although this is the largest value of the two couplings. This highlights that κ does not represent in general a good estimator of the transition.

In the regime of strong coupling, figure 7 shows a discrepancy between the values $\beta_{ij,SEA}$ predicted by equation (3.3) and the average value of $\beta_{ij,REF}$ over the statistical ensemble obtained with the reference calculation. The errors may reach several dozens of decibels. In the strong coupling regime, $\beta_{23,REF}$ can even sometimes take negative values. This is the case for the two values of $\beta_{23,REF}$ labelled negative in figure 7. This indicates that plate 3 has a larger modal energy than plate 2, although the energy is flowing from plate 2 to plate 3.

(iii) Thermal equilibrium

Figure 8 shows the ratios of vibrational temperatures T_2/T_1 and T_3/T_2 versus the stiffness ratio κ. In the weak coupling regime, SEA prediction and the average value of reference calculations agree well. The energy decrease is strong: more than 40 dB from plate 1 to plate 2 and 10 dB less from plate 2 to plate 3 for the lowest values of κ. The exchange of energy is weak, which maintains a large difference in vibrational temperatures. Each plate has reached a state of diffuse field, which means that the energy density is constant over the surface. As by equation (3.1) the modal density is proportional to the area, a constant energy density may be interpreted as a constant local vibrational temperature. Thus, each plate is in thermal equilibrium. But the difference in vibrational temperature from one plate to its neighbour is large. A state of non-equilibrium exists between plates. Such a non-equilibrium state can only be maintained if the loss of energy by exchange is small compared with the internal losses. This is the meaning of Smith's criterion

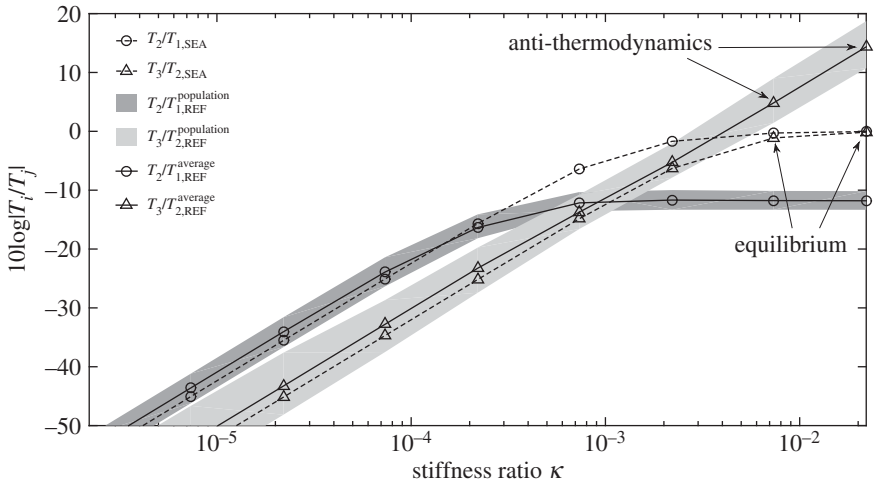

Figure 8. Evolution of $T_j/T_{i,\mathrm{REF}}$ and $T_j/T_{i,\mathrm{SEA}}$ for three plates versus the stiffness ratio κ.

$\eta_{ij} \ll \eta_i$. The state of local equilibrium and global non-equilibrium is therefore the domain where SEA can be applied with a high level of confidence.

For the highest values of the stiffness ratio κ, a discrepancy is observed between SEA and the reference calculation for T_2/T_1 and T_3/T_2. In this regime, SEA tends to predict a state of equilibrium characterized by $T_2/T_1 = T_3/T_2 = 1$ (see the points labelled equilibrium in figure 8). This limit may be easily derived from equations (3.5) and (3.6) by taking the approximations $\eta_2 \ll \eta_{21}$ and $\eta_3 \ll \eta_{32}$ and using for consistency $\eta_{21} n_2 = \eta_{12} n_1$ and $\eta_{32} n_3 = \eta_{23} n_2$. However, the reference calculation gives a difference of 10 dB between plates 1 and 2 and a much greater difference between plates 2 and 3. The state of thermal equilibrium characterized by the equality of vibrational temperatures as predicted by application of SEA to strong coupling is not observed.

Always in the strong coupling regime, the last two points on the right of figure 8 show that the ratio T_3/T_2 is greater than 1. These points correspond to the negative values of β shown in figure 7. A ratio of T_3/T_2 greater than 1 means that vibrational energy flows from the plate with the lowest vibrational temperature to that with the highest temperature. This way of energy flowing from a cold to a hot subsystem may be qualified as anti-thermodynamic since the classical analogy with thermodynamics no longer applies.

4. Conclusion

The main relation of SEA, the coupling power proportionality, states that the mean power between substructures is proportional to the difference in their modal energies with a proportionality factor β. It has been shown that the coupling power proportionality is valid for two oscillators irrespective of the coupling strength. The proportionality coefficient β given by Lyon & Maidanik [3] (equation (2.2)) is correct provided that the 'blocked' natural frequencies are used.

For more than two subsystems, the numerical observations drawn from discrete systems (oscillators) and continuous systems (ensembles of connected plates) are the following.

In the weak coupling regime, the coupling power proportionality is verified well. The values of the proportionality coefficient β for coupled oscillators (equation (2.2)) and for coupled plates (equation (3.3)) give satisfactory results. The energy ratios are therefore well estimated by SEA. In particular, the power always flows from 'hot' to 'cold' subsystems.

In the strong coupling regime, the predictions of the proportionality coefficient β by equations (2.2) and (3.3) are not satisfactory. In particular, the energy ratios of the subsystems are no more well estimated by SEA with these formulae.

The non-constrained identification technique applied to resonators shows that strong coupling is responsible for the appearance of indirect coupling. The indirect coupling loss factors cannot be negligible compared with the direct coupling loss factors and can even dominate them in some situations.

In strong coupling, it may also be that the energy flows from a low modal energy subsystem to a high modal energy subsystem. This inversion of the energy flow from 'cold' to 'hot' subsystems represents a limitation of the classical analogy with thermodynamics. In conclusion, weak coupling is a general requirement for SEA to be applied with confidence.

Data accessibility. This work does not have any experimental data and the Matlab scripts to generate figures of numerical simulations are released as the electronic supplementary material.

Authors' contributions. The ideas presented in this article have been put forward and debated by all authors. All authors have contributed to program the numerical examples, to write the manuscript, and gave final approval for publication.

Competing interests. We have no competing interests.

Funding. This work was supported by the CNRS and Labex CeLyA of Université de Lyon, operated by the French National Research Agency (ANR-10-LABX-0060/ANR-11-IDEX-0007). This support is greatly appreciated.

Acknowledgements. The authors acknowledge the referees for their positive comments and suggestions.

Appendix A

This appendix gives the calculation of the receptance $H_{ij}(\mathbf{r}, \mathbf{s}; \omega)$ of equations (3.8) and (3.9). This is done in two steps.

(a) Single plate

We start by deriving an expression of the receptance $H(\mathbf{r}, \mathbf{s}; \omega)$ of a single plate with resonators.

Let v be the transverse displacement of the plate. The mass per unit area is noted as m, the viscous damping coefficient as c and the bending stiffness as D. If a harmonic force $F \exp(j\omega t)$ is applied at point $\mathbf{s}$, the equation of motion of the plate is

$$-m\omega^2 v + j\omega c v + D\Delta^2 v = F\delta(\mathbf{r} - \mathbf{s}) + \sum_l S_l \delta(\mathbf{r} - \mathbf{s}_l), \tag{A 1}$$

where Δ^2 denotes the bi-Laplacian operator and S_l is the load applied by resonator l at position $\mathbf{s}_l$.

Let u_l be the displacement of resonator l. The governing equation is

$$-M_l\omega^2 u_l + K_l[u_l - v(\mathbf{s}_l)] = 0, \tag{A 2}$$

where the resonator has mass M_l, stiffness K_l and is undamped.

Let ψ_n be the nth 'free' mode (no resonator, no damping) of the plate and ω_n the related eigenfrequency. The modes are orthogonal and are conventionally normalized by $\int \psi_n(\mathbf{r})\psi_m(\mathbf{r})\mathrm{d}\mathbf{r} = \delta_{nm}$. For simply supported edges, the nth mode referred to by two integers $n = (p, q)$ is

$$\psi_n(x, y) = \frac{2}{\sqrt{ab}} \sin\left(p\pi \frac{x}{a}\right) \sin\left(q\pi \frac{y}{b}\right) \quad p, q = 1, 2, \ldots, \tag{A 3}$$

where the plate has length a and width b.

Since the dissipation in equation (A 1) is modelled by a viscous damping coefficient proportional to the mass density, the displacement field $v(\mathbf{r})$ of the damped plate may be developed in the series of the undamped modes

$$v(\mathbf{r}) = \sum_n A_n \psi_n(\mathbf{r}). \tag{A 4}$$

Substituting into the governing equation (A 1) and using the orthogonality property of normal modes give

$$v(\mathbf{r}) = \sum_n \frac{F_n \psi_n(\mathbf{r})}{m(\omega_n^2 + j\Delta\omega - \omega^2)}, \tag{A 5}$$

where $\Delta = c/m$ is the half-power bandwidth of all modes and the modal force F_n is

$$F_n = F\psi_n(\mathbf{s}) + \sum_l S_l \psi_n(\mathbf{s}_l). \tag{A 6}$$

Furthermore, the reaction of the lth resonator is

$$S_l = K_l[u_l - v(\mathbf{s}_l)]. \tag{A 7}$$

The receptance of the plate with resonators is $H(\mathbf{r}, \mathbf{s}; \omega) = v(\mathbf{r})$, where a unit force $F = 1$ has been substituted. Combining (A 5)–(A 7), this may be written

$$H(\mathbf{r}, \mathbf{s}; \omega) = H^0(\mathbf{r}, \mathbf{s}; \omega) + \sum_l K_l[u_l - v(\mathbf{s}_l)]H^0(\mathbf{r}, \mathbf{s}_l; \omega), \tag{A 8}$$

where

$$H^0(\mathbf{r}, \mathbf{s}; \omega) = \sum_n \frac{\psi_n(\mathbf{s})\psi_n(\mathbf{r})}{m(\omega_n^2 + j\Delta\omega - \omega^2)} \tag{A 9}$$

is the receptance of the 'free' plate. The problem therefore reduces to the determination of the unknowns $v(\mathbf{s}_l)$ and u_l.

They are obtained by applying (A 8) and at points $\mathbf{r} = \mathbf{s}_l$. This gives

$$v(\mathbf{s}_l) = H^0(\mathbf{s}_l, \mathbf{s}; \omega) + \sum_{l'} K_{l'}[u_{l'} - v(\mathbf{s}_{l'})]H^0(\mathbf{s}_l, \mathbf{s}_{l'}; \omega). \tag{A 10}$$

Equation (A 2) gives the second equation

$$u_l = K_l H_l(\omega) v_i(\mathbf{s}_l), \tag{A 11}$$

where $H_l(\omega) = 1/(-M_l\omega^2 + K_l)$ denotes the receptance of resonator l.

The method consists in first determining the unknowns $v(\mathbf{s}_l)$ and u_l by solving the set of linear equations (A 10) and (A 11), and second in calculating the receptance $H(\mathbf{r}, \mathbf{s}; \omega)$ at any point $\mathbf{r}$ with equation (A 8).

(b) Coupled plates

This subsection gives the receptance $H_{ij}(\mathbf{r}, \mathbf{s}; \omega)$ of N plates coupled through springs of stiffness K. Each plate is covered by mass-spring resonators and has an 'isolated' receptance (no coupling) noted $H_i(\mathbf{r}, \mathbf{s}; \omega)$ which may calculated by the method of the previous subsection.

Assuming that a harmonic point load $F\exp(j\omega t)$ is applied to plate j at point $\mathbf{s}$, the displacement in plate i at point $\mathbf{r}$ is

$$v_i(\mathbf{r}) = F\delta_{ij}H_i(\mathbf{r}, \mathbf{s}; \omega) + \sum_k R_{ik}H_i(\mathbf{r}, \mathbf{r}_{ik}; \omega), \tag{A 12}$$

where R_{ik} is the reaction applied by plate k onto plate i through the coupling spring at position $\mathbf{r}_{ik}$. The presence of δ_{ij} on the right-hand side means that the external load term is present only for plate j.

The reaction R_{ik} is

$$R_{ik} = K[v_k(\mathbf{r}_{ki}) - v_i(\mathbf{r}_{ik})]. \tag{A 13}$$

Therefore, by substituting (A 13) into (A 12) and setting $F = 1$, the receptance of the coupled plates $H_{ij}(\mathbf{r}, \mathbf{s}; \omega) = v_i(\mathbf{r})$ is

$$H_{ij}(\mathbf{r}, \mathbf{s}; \omega) = \delta_{ij} H_i(\mathbf{r}, \mathbf{s}; \omega) + \sum_k K[v_k(\mathbf{r}_{ki}) - v_i(\mathbf{r}_{ik})] H_i(\mathbf{r}, \mathbf{r}_{ik}; \omega). \tag{A 14}$$

The unknowns $v_i(\mathbf{r}_{ik})$ are determined by setting $\mathbf{r} = \mathbf{r}_{ik}$ into equation (A 14). This yields

$$v_i(\mathbf{r}_{ik}) = \delta_{ij} H_i(\mathbf{r}_{ik}, \mathbf{s}; \omega) + \sum_{k'} K[v_{k'}(\mathbf{r}_{k'i}) - v_i(\mathbf{r}_{ik'})] H_i(\mathbf{r}, \mathbf{r}_{ik'}; \omega). \tag{A 15}$$

The method consists in first solving the set of linear equations (A 15) in unknowns $v_i(\mathbf{r}_{ik})$ and then computing the receptance of the coupled plates with (A 14).

For instance, for the three plates in figure 5, the first spring is attached at $\mathbf{r}_{12}$ on plate 1 and $\mathbf{r}_{21}$ on plate 2. The second spring is attached at points $\mathbf{r}_{23}$ on plate 2 and $\mathbf{r}_{32}$ on plate 3. The excited plate is $j = 1$. The three receptances $H_{i1}(\mathbf{r}, \mathbf{s}; \omega)$ form a column vector $\mathbf{H} = (H_{11}, H_{21}, H_{31})^{\mathrm{T}}$ given by

$$\mathbf{H}(\mathbf{r}, \mathbf{s}; \omega) = K\Psi(\mathbf{r})\mathbf{V} + \mathbf{F}(\mathbf{r}), \tag{A 16}$$

where $\mathbf{V} = (v_1(\mathbf{r}_{12}), v_2(\mathbf{r}_{21}), v_2(\mathbf{r}_{23}), v_3(\mathbf{r}_{32}))^{\mathrm{T}}$, $\mathbf{F}(\mathbf{r}) = (\Phi_1(\mathbf{s}, \mathbf{r}), 0, 0)^{\mathrm{T}}$ and

$$\Psi(\mathbf{r}) = \begin{pmatrix} -\Phi_1(\mathbf{r}_{12}, \mathbf{r}) & \Phi_1(\mathbf{r}_{12}, \mathbf{r}) & 0 & 0 \\ \Phi_2(\mathbf{r}_{21}, \mathbf{r}) & -\Phi_2(\mathbf{r}_{21}, \mathbf{r}) & -\Phi_2(\mathbf{r}_{23}, \mathbf{r}) & \Phi_2(\mathbf{r}_{23}, \mathbf{r}) \\ 0 & 0 & \Phi_3(\mathbf{r}_{32}, \mathbf{r}) & -\Phi_3(\mathbf{r}_{32}, \mathbf{r}) \end{pmatrix}. \tag{A 17}$$

The unknowns are determined by the system

$$(\mathbf{I} + K\Phi)\mathbf{V} = \mathbf{F}_0, \tag{A 18}$$

where $\mathbf{I}$ is the 4×4 identity matrix and $\mathbf{F}_0 = (\Phi_1(\mathbf{s}, \mathbf{r}_{12}), 0, 0, 0)^{\mathrm{T}}$. The matrix Φ is

$$\Phi = \begin{pmatrix} \Phi_1(\mathbf{r}_{12}, \mathbf{r}_{12}) & -\Phi_1(\mathbf{r}_{12}, \mathbf{r}_{12}) & 0 & 0 \\ -\Phi_2(\mathbf{r}_{21}, \mathbf{r}_{21}) & \Phi_2(\mathbf{r}_{21}, \mathbf{r}_{21}) & \Phi_2(\mathbf{r}_{23}, \mathbf{r}_{21}) & -\Phi_2(\mathbf{r}_{23}, \mathbf{r}_{21}) \\ -\Phi_2(\mathbf{r}_{21}, \mathbf{r}_{23}) & \Phi_2(\mathbf{r}_{21}, \mathbf{r}_{23}) & \Phi_2(\mathbf{r}_{23}, \mathbf{r}_{23}) & -\Phi_2(\mathbf{r}_{23}, \mathbf{r}_{23}) \\ 0 & 0 & -\Phi_3(\mathbf{r}_{32}, \mathbf{r}_{32}) & \Phi_3(\mathbf{r}_{32}, \mathbf{r}_{32}) \end{pmatrix}. \tag{A 19}$$

The receptances are therefore given by equation (A 16) at all points $\mathbf{r}$ for any excitation point $\mathbf{s}$ where the unknowns are obtained by solving equation (A 18).

References

1. Lyon RH, DeJong R. 1995 *Theory and application of statistical energy analysis*. Boston, MA: Butterworth-Heinemann.
2. Le Bot A. 2015 *Foundation of statistical energy analysis in vibroacoustics*. Oxford, UK: Oxford University Press.
3. Lyon RH, Maidanik G. 1962 Power flow between linearly coupled oscillators. *J. Acoust. Soc. Am.* **34**, 623–639. (doi:10.1121/1.1918177)
4. Newland DE. 1966 Calculation of power flow between coupled oscillators. *J. Sound Vib.* **3**, 262–276. (doi:10.1016/0022-460X(66)90095-2)
5. Fahy F. 1994 Statistical energy analysis: a critical overview. *Phil. Trans. R. Soc. Lond. A* **346**, 431–447. (doi:10.1098/rsta.1994.0027)
6. Burroughs C, Fisher R, Kern F. 1997 An introduction to statistical energy analysis. *J. Acoust. Soc. Am.* **101**, 1779–1789. (doi:10.1121/1.418074)
7. Culla A, Sestieri A. 2006 Is it possible to treat confidentially SEA the wolf in sheep's clothing? *Mech. Syst. Sig. Proc.* **20**, 1372–1399. (doi:10.1016/j.ymssp.2005.02.007)
8. Sestieri A, Carcaterra A. 2013 Vibroacoustic: the challenges of a mission impossible? *Mech. Syst. Sig. Proc.* **34**, 1–18. (doi:10.1016/j.ymssp.2012.08.010)

9. Lecomte C. 2014 A frequency averaging framework for the solution of complex dynamic systems. *Proc. R. Soc. A* **470**, 20130743. (doi:10.1098/rspa.2013.0743)
10. Lafont T, Totaro N, Le Bot A. 2014 Review of statistical energy analysis hypotheses in vibroacoustics. *Proc. R. Soc. A* **470**, 1471–2946. (doi:10.1098/rspa.2013.0515)
11. Le Bot A. 2017 Entropy in sound and vibration: towards a new paradigm. *Proc. R. Soc. A.* **473**, 20160602. (doi:10.1098/rspa.2016.0602)
12. Fahy F, Yao d-Y. 1987 Power flow between non-conservatively coupled oscillators. *J. Sound Vib.* **114**, 1–11. (doi:10.1016/S0022-460X(87)80227-4)
13. Scharton TD, Lyon RH. 1968 Power flow and energy sharing in random vibration. *J. Acoust. Soc. Am.* **43**, 1332–1343. (doi:10.1121/1.1910990)
14. Sun JC, Wang C, Sun ZH. 1996 Power flow between three series coupled oscillators. *J. Sound Vib.* **189**, 215–229. (doi:10.1006/jsvi.1996.0016)
15. Woodhouse J. 1981 An approach to the theoretical background of statistical energy analysis applied to structural vibration. *J. Acoust. Soc. Am.* **69**, 1695–1709. (doi:10.1121/1.385949)
16. Keane AJ, Price WJ. 1987 Statistical energy analysis of strongly coupled systems. *J. Sound Vib.* **117**, 263–286. (doi:10.1016/0022-460X(87)90545-1)
17. Finnveden S. 2011 A quantitative criterion validating coupling power proportionality in statistical energy analysis. *J. Sound Vib.* **330**, 87–109. (doi:10.1016/j.jsv.2010.08.003)
18. Smith PW. 1979 Statistical models of coupled dynamical systems and the transition from weak to strong coupling. *J. Acoust. Soc. Am.* **65**, 695–698. (doi:10.1121/1.382481)
19. Langley RS. 1989 A general derivation of the statistical energy analysis equations for coupled dynamic systems. *J. Sound Vib.* **135**, 499–508. (doi:10.1016/0022-460X(89)90702-5)
20. Fahy F, James PP. 1996 A study of the kinetic energy impulse as an indicator of strength of coupling between sea subsystems. *J. Sound Vib.* **190**, 363–386. (doi:10.1006/jsvi.1996.0069)
21. Mace BR. 1993 The statistical energy analysis of two continuous one-dimensional subsystems. *J. Sound Vib.* **166**, 429–461. (doi:10.1006/jsvi.1993.1305)
22. Mace B, Ji L. 2007 The statistical energy analysis of coupled sets of oscillators. *Proc. R. Soc. A* **463**, 1359–1377. (doi:10.1098/rspa.2007.1824)
23. Finnveden S. 1995 Ensemble averaged vibration energy flows in a three element structure. *J. Sound Vib.* **187**, 495–529. (doi:10.1006/jsvi.1995.0538)
24. Mace B. 2003 Statistical energy analysis, energy distribution models and system modes. *J. Sound Vib.* **264**, 391–409. (doi:10.1016/S0022-460X(02)01201-4)
25. Mace B. 2005 Statistical energy analysis: coupling loss factors, indirect couplings and system modes. *J. Sound Vib.* **279**, 141–170. (doi:10.1016/j.jsv.2003.10.040)
26. Bies D, Hamid S. 1980 In situ determination of loss and coupling loss factors by the power injection method. *J. Sound Vib.* **90**, 187–204. (doi:10.1016/0022-460X(80)90595-7)
27. Newland DE. 1968 Power flow between a class of coupled oscillators. *J. Acoust. Soc. Am.* **43**, 553–559. (doi:10.1121/1.1910865)
28. Le Bot A. 2007 Derivation of statistical energy analysis from radiative exchanges. *J. Sound Vib.* **300**, 763–779. (doi:10.1016/j.jsv.2006.08.033)
29. Le Bot A, Cotoni V. 2010 Validity diagrams of statistical energy analysis. *J. Sound Vib.* **329**, 221–235. (doi:10.1016/j.jsv.2009.09.008)